A NEW TRAVELING INTERFEROMETRIC SCHEME FOR THE APS UPGRADE OF THE 2-ID BIONANOPROBE*

S. Bean, S. Chen, T. Graber[†], C. Jacobsen, B. Lai, E. Maxey,
T. Mooney, C. Preissner, X. Shi, D. Shu, J. Tan, M. Wojcik
Advanced Photon Source, Argonne National Laboratory, Lemont, IL 60439, USA
[†] Deceased April 29, 2021

Abstract

The Advanced Photon Source (APS) at Argonne National Laboratory (ANL) is being upgraded to a multi-bend achromat (MBA) lattice storage ring which will increase brightness and coherent flux by several orders of magnitude. As part of this upgrade a total of 15 beamlines were selected to be enhanced to take advantage of the new source – these are designated as "Enhanced Beamlines". Among these is the enhancement to 2-ID, which includes an upgrade and move of the existing Bionanoprobe (BNP) from 9-ID [1]. This instrument will become the second generation Bionanoprobe II (BNP-II) with intent of studying cryogenic samples with sub-10 nm resolution. This upgrade requires a high performing metrology configuration and design to achieve the desired spatial resolution while adapting to the various constraints of the instrument. The cryogenic sample environment and detection constraints offer significant challenges for implementing a metrology scheme. In this paper we report on the new traveling interferometer configuration proposed for BNP-II.

INTRODUCTION

The unique challenge for implementing metrology for BNP-II is the cryogenic sample environment. The desired instrument resolution lends to a design that measures positions as close to the actual cryogenic sample as is feasible. This must be accomplished for a sample that translates in X/Y/Z directions and rotates around a vertical (Y) axis.

Recent developments at Swiss Light Source have resulted robust metrology solutions for rotating samples such as passive anti rotation and tracking interferometer designs [2-4]. These schemes were considered for BNP-II. Implementation would come with a unique set of challenges for BNP-II give the space limitations in the XZ plane, and the desire to measure a reference object which is at cryogenic temperatures.

Our design incorporates a new traveling interferometer concept for the sample as shown in Figure 1. A traveling interferometer platform tracks a cryogenic cylindrical reference in the horizontal plane and is decoupled from the other degrees of freedom (DOF) of the sample stage stack. A set of stationary global interferometers measure information both from the reference and from the traveling platform.

It is worth note that the desired instrument resolution is pushing the limits on off-the-shelf interferometer hardware. Periodic error is considered for the design but is not discussed further [5].
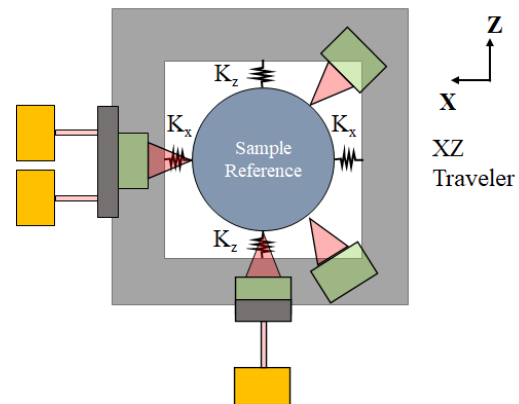

Figure 1: The coupled traveling interferometer concept. The traveling XZ travler support is coupled to the sample reference on the X and Z degrees of freedom, while decoupled in the other degrees of freedom. Focused traveling interferometers (green) and global stationary interferometers (gold) are depicted.

SCANNING & METROLOGY METHODOLOGY

The following numbered items represent the most critical and complex set of requirements of the metrology strategies for BNP-II:

1. The metrology system must provide position information below 2 nm in order to achieve a 10 nm fluorescence resolution for the instrument.
2. The cryogenic sample will be continuously scanned while the optics are stationary during measurement.
3. The metrology scheme must be able to measure re-positioning of the sample through translations and one main vertical rotation axis.
4. The sample metrology reference optic and the sample should be intimately coupled.
5. The metrology must incorporate relative measurements between the optic and sample positions for both positioning and scanning.
6. The metrology should be non-intrusive to the nearby XZ (horizontal) plane of the sample to allow for signal collection, beam-conditioning optics, and thermal shielding.

Precision mechanics

Nano-Positionning

METROLOGY RERERENCE DESIGN

A cylindrical metrology reference is selected for this configuration as shown in Figure 2. The radial and top surface are to be made to optically acceptable form and surface finish. The resultant metrology surfaces of the reference must be characterized, as they will be needed for position controls corrections.
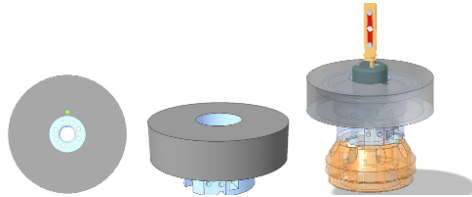

Figure 2: The sample optical reference top and isometric view (left). Sample mount design (right) including from bottom up the warm kinematic interface, cryogenic reference, and sample loading interface.

TRAVELING CONFIGURATION

The proposed sample scanning stack configuration is shown in Figure 3. A vertical fast scanning axis is implemented above the traveler mechanics (TM). All other degrees of freedom are below the TM, including the slow scanning XZ stage.
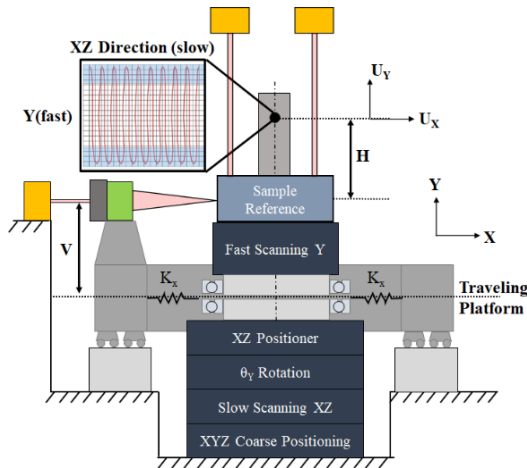

Figure 3: Schematic showing how the configuration of the interferometers, traveleing platform (TP), traveling mechanics (TM), and sample stages can be configured in order to have the focused interferometers track the XZ position of the reference while also allowing for uncoupled fast vertical scanning to occure. The fly scan strategy is depicted for the sample. The fast direction is vertical (Y), while the slow direction is in an arbitrary direction in the XZ plane. The traveling platform is supported by an external planar XZ bearing.

BNP-II METROLOGY CONFIGURATION

The proposed metrology configuration (see Figure 4) consists of 16 interferometers situated in a strategic way to measure all the information required to know the relative position of the optic and sample. A summary of what interferometers are measuring which DOF is shown in Table 1.
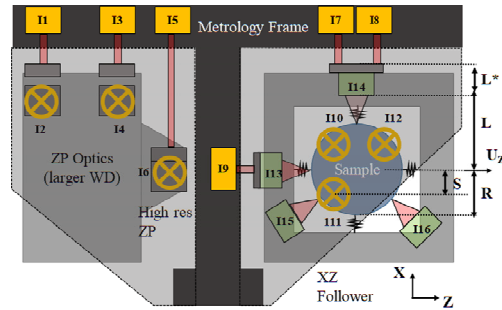

Figure 4: Schematic showing complete metrology configuration for relative sample and optic measurement. Gold indicates nonmoving measurements with respect to the global metrology frame. An "X" indicates the measurement is from above to the respective reference surface. Green indicates a traveling interferometer. The shape of the interferometer beam is either collimated (straight) or focused (angled). Z is the beam direction.

Table 1: Table showing which interferometers are measuring which DOF of the optic and sample.

Measured Degrees of Freedom of Interferometers			
Interferometer/s	Measured (Or Calculated*) Degrees of Freedom	Measurement From	Metrology Head Type
I1 & I3	Coarse Optic X, θ_Y	Reference Frame	Collimated
I2 & I4	Coarse Optic Y, θ_X	Reference Frame	Collimated
I5	High Res. Optic X	Reference Frame	Collimated
I6	High Res. Optic Y	Reference Frame	Collimated
I7 & I8	Sample Follower X, θ_Y	Reference Frame	Collimated
I9	Sample Follower Z	Reference Frame	Collimated
I10 & I11 & I12	Sample Y, θ_X, θ_Z	Reference Frame	Collimated
I13	Sample Z	Sample Follower	Focused
I14	Sample X	Sample Follower	Focused
I15 & I16*	N/A, For Form Characterization	Sample Follower	Focused

REFERENCE ERROR ANALYSIS

Some geometric first order errors are considered between the reference optic and the interferometers. This includes the traveler X and Z interferometers (I13, I14), along with the global Y interferometers (I10, I11, I12). Table 2 is a summary of the parasitic error motion of the reference, the corresponding interferometer change and actual sample motion.

Table 2: Table showing the optic errors and the corresponding geometric changes in metrology and sample position. A "/" indicates the respective equations for the x or z direction.

Optic Error Motion	Change in Traveling Interferometer (T), Global Interferometer (G)	Actual Sample Change (U)
$\delta x/z$	$T_{X/Z} = \delta x/z$ $T_{Z/X} = R - \sqrt{R^2 - \delta x/z^2}$	$U_{X/Z} = \delta x/z$
$\delta \theta_{X/Z}$	$T_{Z/X} = R\left(1 - \dfrac{1}{\cos(\delta\theta_{X/Z})}\right) \approx 0$ $G_{Y1} = (S)\delta\theta_{X/Z}$ $G_{Y2} = -(S)\delta\theta_{X/Z}$ $G_{Y3} = -(S)\delta\theta_{X/Z}$	$U_{Z/X} = (H)\delta\theta_{X/Z}$ $U_Y = (H)\dfrac{\delta\theta_{X/Z}^{2}}{4}$ $U_{\theta_{X/Z}} = \delta\theta_{X/Z}$
$\delta\theta_Y$	Blind	$U_{\theta_Y} = \delta\theta_Y$

The following conclusions are made:

1. The X & Z interferometers don't discern actual sample displacements U_X and U_Z <u>caused</u> by angular errors of the optic.
2. U_X and U_Z changes <u>caused</u> by angular errors must be calculated; they are not measured directly.
3. The X and Z measurements are coupled.

The first two conclusions are a result of not measuring the reference at the work point, which some designed metrology schemes have taken care to implement [6]. The last conclusion is discussed next.

XZ COUPLED EQUATIONS

The measurement coupling of the X and Z reference DOF are depicted in Figure 5. When calculating the true δx and δz change of the optic with respect to obtained signals, the following relationships can be derived:

$$\text{INT1} = \boldsymbol{\delta x} + R - \sqrt{R^2 - \boldsymbol{\delta z^2}}$$
$$\text{INT2} = \boldsymbol{\delta z} + R - \sqrt{R^2 - \boldsymbol{\delta x^2}}$$

This system of equations can be solved iteratively. To determine the total change of the actual sample position in the XZ plane, the result is added to any additional XZ changes from the global Y interferometers. However, if the radius term R is much larger than the errors, these interferometers then give a direct measurement of the reference X and Z.
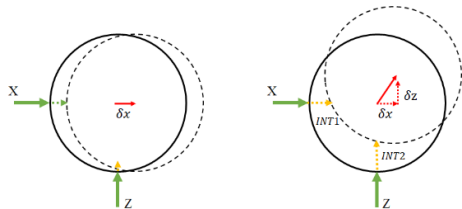

Figure 5: Schematic showing X error of the fast-scanning optic (left), and a combined error of the optic (right).

TRAVELER ERROR ANALYSIS

As was done for the reference, a geometric error study was done for the traveler and is summarized in Table 3.

Table 3. Table showing the traveler errors and the corresponding geometric changes in metrology and sample position. A "/" indicates the respective direction equation and terms.

Traveler Error Motion	Change in Traveling Interferometer (T), Global Interferometer (G)	Actual Sample Change (U)
$\delta x/z$	$T_{X/Z} = \delta x/z$ $T_{Z/X} = R - \sqrt{R^2 - \delta x/z^2}$ $G_{X/Z} = -\delta x/z$	None
$\delta\theta_{X/Z}$	$T_{Z/X} = \left(\text{L} - \text{V}\,\delta\theta_{X/Z} - R\right)\left(\sqrt{\delta\theta_{X/Z}^2 + 1} - 1\right)$ $T_{X/Z} = \text{R} - \sqrt{R^2 - V\delta\theta_{X/Z}^2}$ $G_{Z/X} = V\delta\theta_{X/Z} - \delta\theta_{X/Z}^2(L + L^*)$	None
$\delta\theta_Y$	$G_{X1} = -G_{X2}$	None

The following conclusions are made:

1. The X & Z traveler interferometers see similar coupling as if the reference has moved, however now there is no sample motion. This is to be compensated by the global interferometer change.
2. The sum of the global and traveler interferometer response from angular traveler changes is not zero. This cannot be compensated by measurements unless more opposing interferometers are utilized.

Based on the error analysis of Table 3, and given a set of characteristic lengths for a feasible design, 50 μrad change of the traveler leads to about 0.1 nm error in a measurement. As the traveler rotates, the global and traveling interferometers respond in an opposite manner, but do not completely cancel, thus leading to this smalls sensitivity. This amount of error and sensitivity should be accounted for in the error budget when guiding mecahnics for the follower are being chosen.

TRAVELER RESONANCE CONSIDERATIONS

Assuming the traveler planar coupling stiffnesses is much lower than typical stage bearings, the twice repeated eigenvalue for two directions of Figure 1 is given as

$$\omega = \sqrt{2K/m}, \text{where } K = K_X = K_Z$$

where m is the mass of the traveler platform. The traveler mass must be chosen appropriately with respect to the stiffness coupling in the XZ plane versus the desired scanning frequency of the instrument to avoid resonance.

PROPOSED DESIGN CONCEPT

The design concept for the traveling interferometer scheme is shown in Figure 6. The central stack as seen in the exploded view is then supported by the other DOF below as shown in Figure 3.
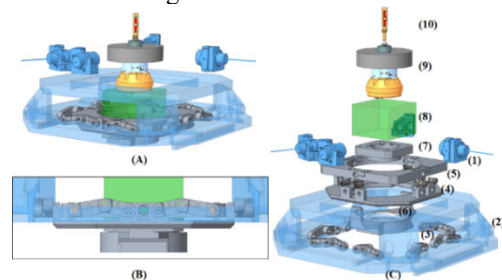

Figure 6: A schematic showing the design concept for the traveling inteferometer. A- overview, B- front view of vertical compliant link interface, C- exploded view showing 1- traveling interfereometer, 2- traveling frame, 3- vertical compliant links, 4/5/6- tip tilt mechanism with buried radial bearing set, 7- radial bearing preload and stage inteface plate, 8- scanning Y stage space claim, 9- sample reference, 10- sample mount.

CONCLUSIONS

A new metrology configuration is proposed for BNP-II to measure a cryogenic reference. The first analysis indicates there is potential to achieve the performance goals of this instrument. Important design considerations were discussed. The design and control strategies will be further refined and completed.

REFERENCES

[1] S. Chen *et al*., "The Bionanoprobe: Hard X-ray fluorescence nanoprobe with cryogenic capabilities," *J. Synchrotron Radiat*., vol. 21, pp. 66-75, 2014. `10.1107/S1600577513029676`

[2] M. Holler, J. Raabe., "Error motion compensating tracking interferometer for the position measurement of objects with rotational degree of freedom," *Opt. Eng*., vol. 54, no. 5, p. 054101, May 2015. `https://doi.org/10.1117/1.OE.54.5.054101`

[3] M. Holler, M. Odstrcil, M. Guizar-Sicairos *et al*., "Three-dimensional imaging of integrated circuits with macro- to nanoscale zoom," *Nat. Electron.* vol. 2, pp. 464–470, 2019. `https://doi.org/10.1038/s41928-019-0309-z`

[4] M. Holler, J. Raabe, A. Diaz, M. Guizar-Sicairos, C. Quitmann, A. Menzel, and O. Bunk, "An instrument for 3D x-ray nano-imaging," *Rev. Sci. Instrum*., vol. 83, p. 073703, 2012, `https://doi.org/10.1063/1.4737624`

[5] K. Turner, F. Quacquarelli, P.F. Braun, C. Savio, and K. Karrai, "Fiber-based distance sensing interferometry," *Appl. Opt*., vol. 54, pp. 3051-3063, 2015. `10.1364/AO.54.003051`

[6] F. Villar and L. Ducotté, "L8–Introduction to Precision Positioning Systems," presented at ESRF MEDSI School 2, Grenoble, France, 2019, unpublished.